



STRUCTURAL
CHEMISTRY

Volume 78 (2022)

Supporting information for article:

Investigating pair distribution function use in analysis of nanocrystalline hydroxyapatite- and carbonate-substituted hydroxyapatite

Emily L. Arnold, Dean S. Keeble, J. P. O. Evans, Charlene Greenwood and Keith D. Rogers

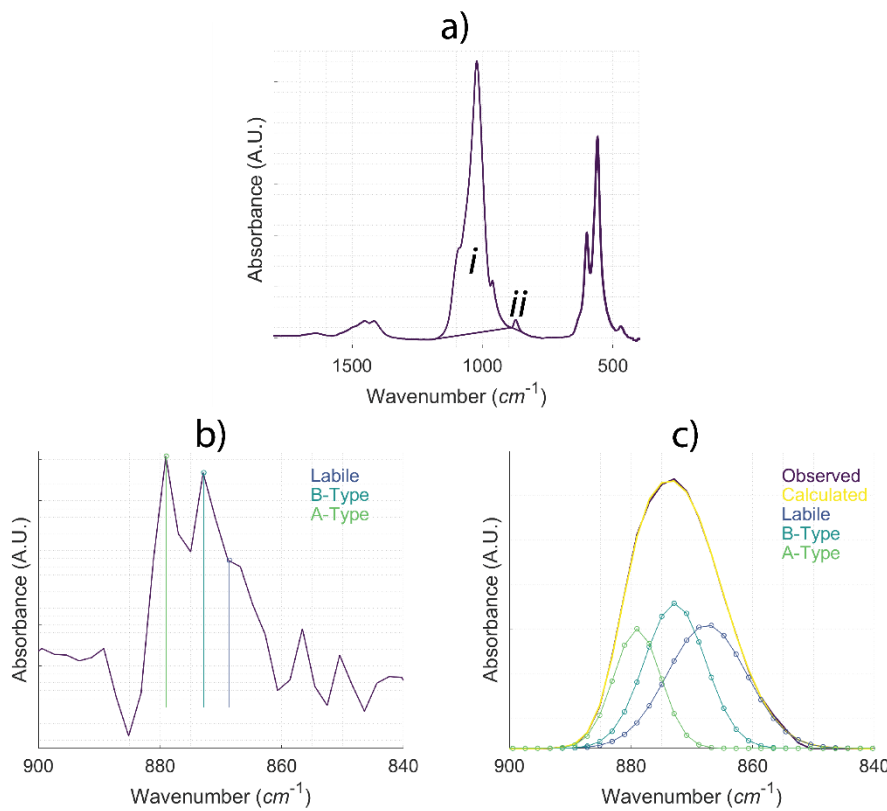


Figure S1 Example of FTIR analysis. a) shows a section of the spectrum with *i* and *ii* representing the $\text{v}_1\text{v}_3\text{PO}_4^{3-}$ and the $\text{v}_2\text{CO}_3^{2-}$ absorption bands respectively. b) shows the deconvoluted spectrum between 900 cm^{-1} and 840 cm^{-1} . c) shows the result of fitting three peaks to the $\text{v}_2\text{CO}_3^{2-}$ absorption band using PeakFit4 (SigmaPlot).

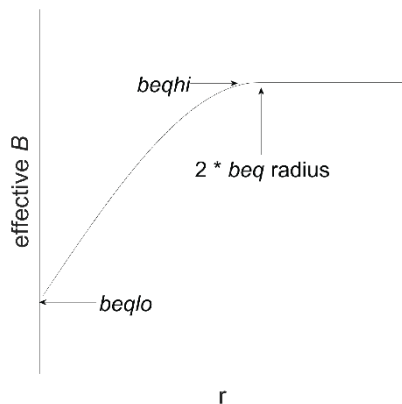


Figure S2 Effective temperature factor using spherical function.

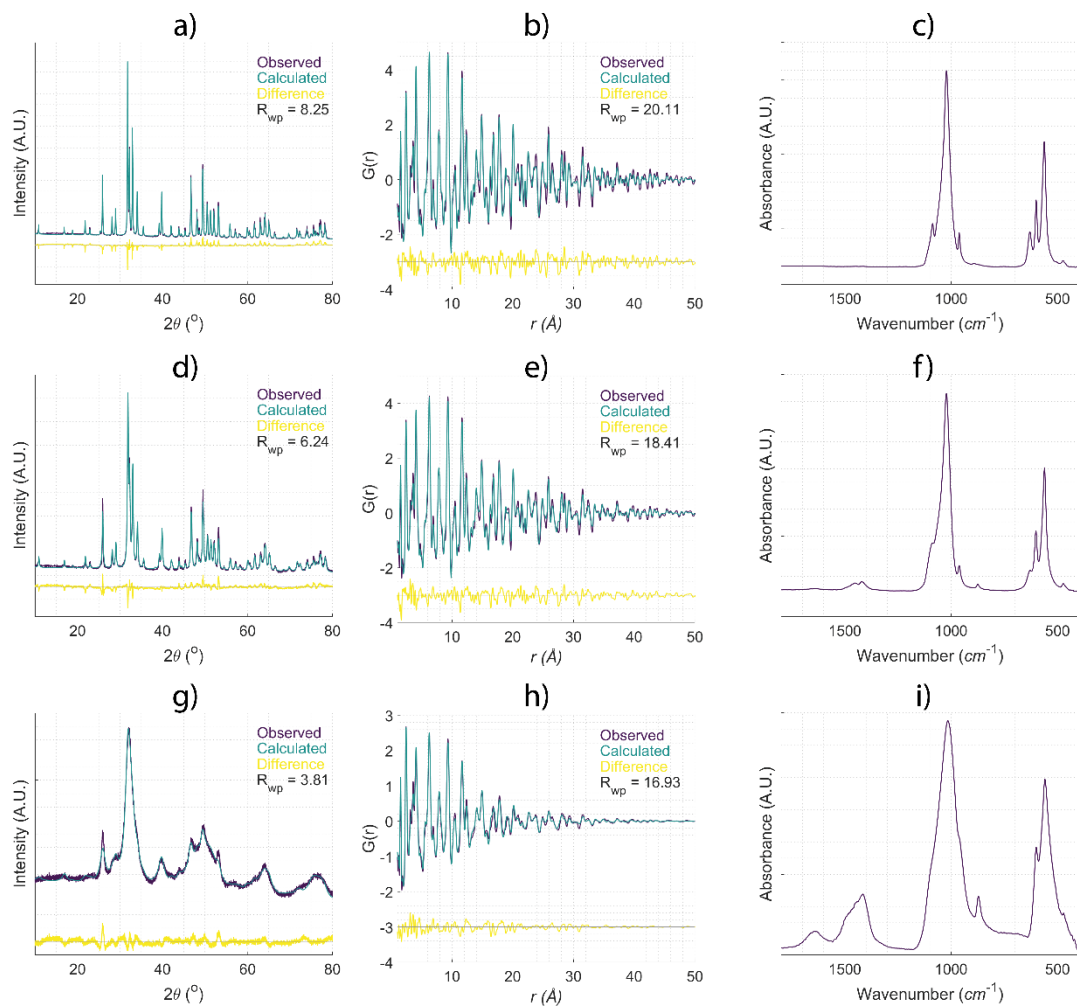


Figure S3 Examples. NIST SRM 2910b a) Rietveld refinement, b) real-space refinement and c) FTIR spectrum. High temperature (highly crystalline) synthesised 1.24 wt% d) Rietveld refinement, e) real-space refinement and f) FTIR spectrum. Low temperature (nanocrystalline) synthesised 7.98 wt% g) Rietveld refinement, h) real-space refinement and i) FTIR spectrum.

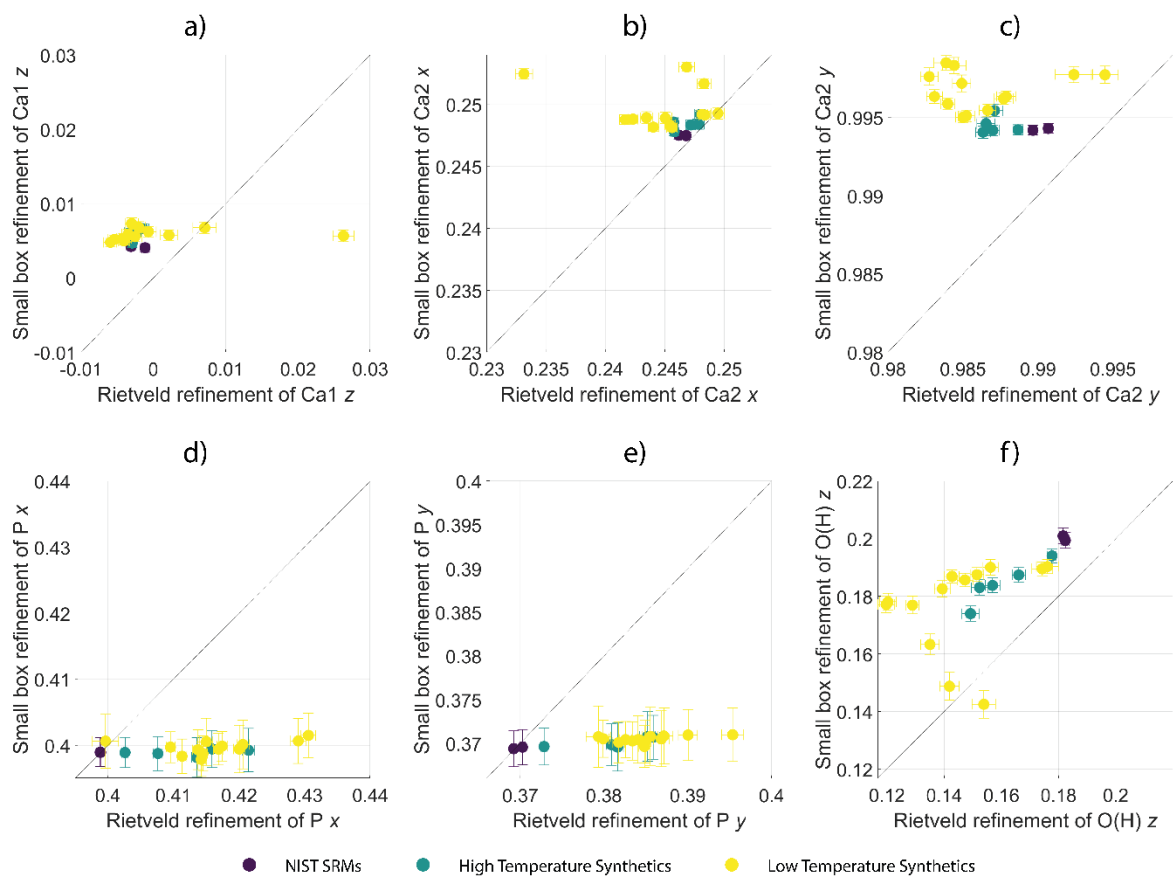


Figure S4 Comparison of fractional coordinates calculated from both Rietveld refinement of Bragg data and real-space refinement of PDF data: *a*) Ca1 z , *b*) Ca2 x , *c*) Ca2 y , *d*) P x , *e*) P y and *f*) O(H) z . Error bars represent estimated standard deviation.

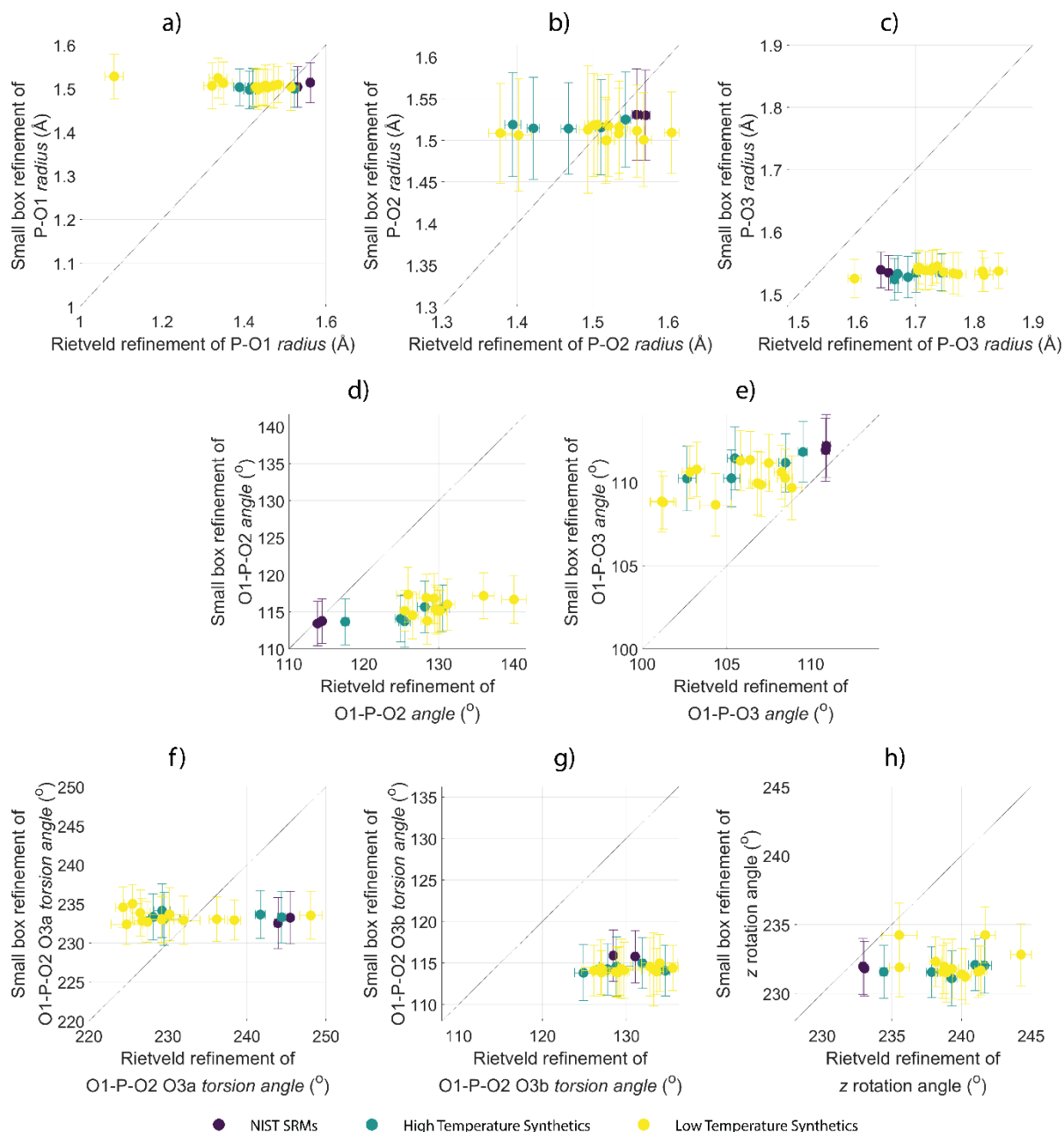


Figure S5 Comparison of rigid body parameters calculated from both Rietveld refinement of Bragg data and real-space refinement of PDF data: *a*) P-O1 bond distance, *b*) P-O2 bond distance, *c*) P-O3 bond distance, *d*) O1-P-O2 angle, *e*) O1-P-O3 angle, *f*) O1-P-O2 O3a torsion angle, *g*) O1-P-O2 O3b torsion angle and *h*) *z* rotation angle. Error bars represent estimated standard deviation.

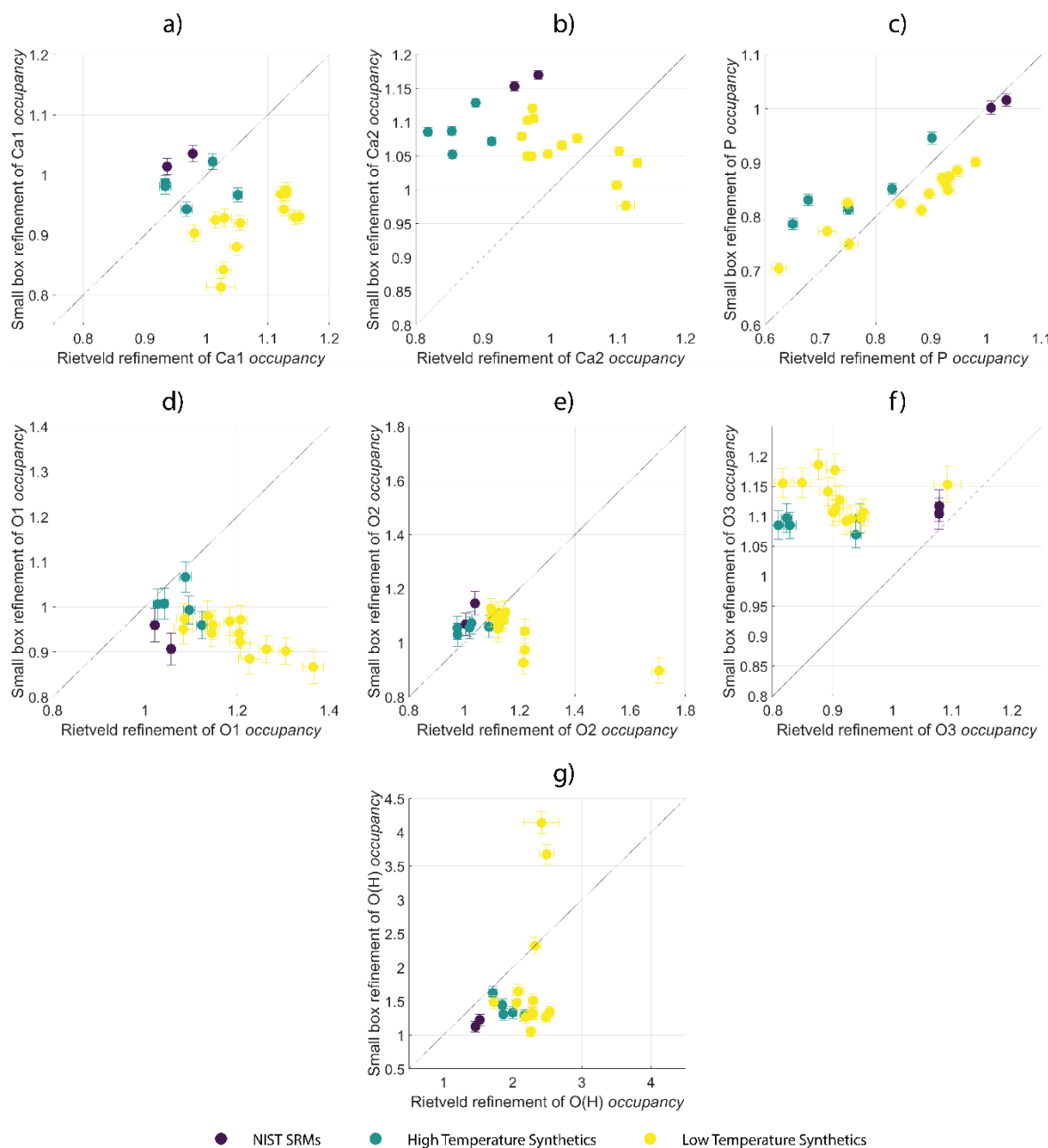


Figure S6 Comparison of occupancies calculated from both Rietveld refinement of Bragg data and real-space refinement of PDF data: *a*) Ca1 occupancy, *b*) Ca2 occupancy, *c*) P occupancy, *d*) O1 occupancy, *e*) O2 occupancy, *f*) O3 occupancy and *g*) O(H) occupancy. Error bars represent estimated standard deviation.

Table S1 Results of linear regression between expected P occupancy and the experimental P occupancy for both Rietveld and real-space refinements.

	Rietveld Refinement	Real-space Refinement
p	0.001	0.001
R^2 (adjusted)	0.62	0.72
Correlation	0.80	0.86

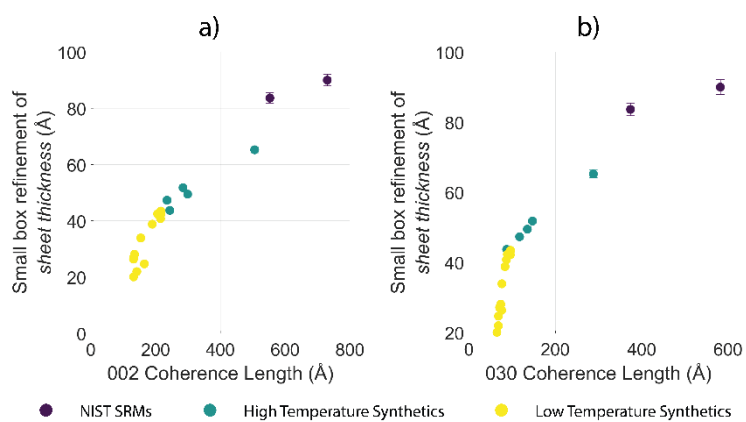


Figure S7 Comparison of sheet thickness and *a*) 002 CL and *b*) 030 CL. Error bars represent estimated standard deviation.

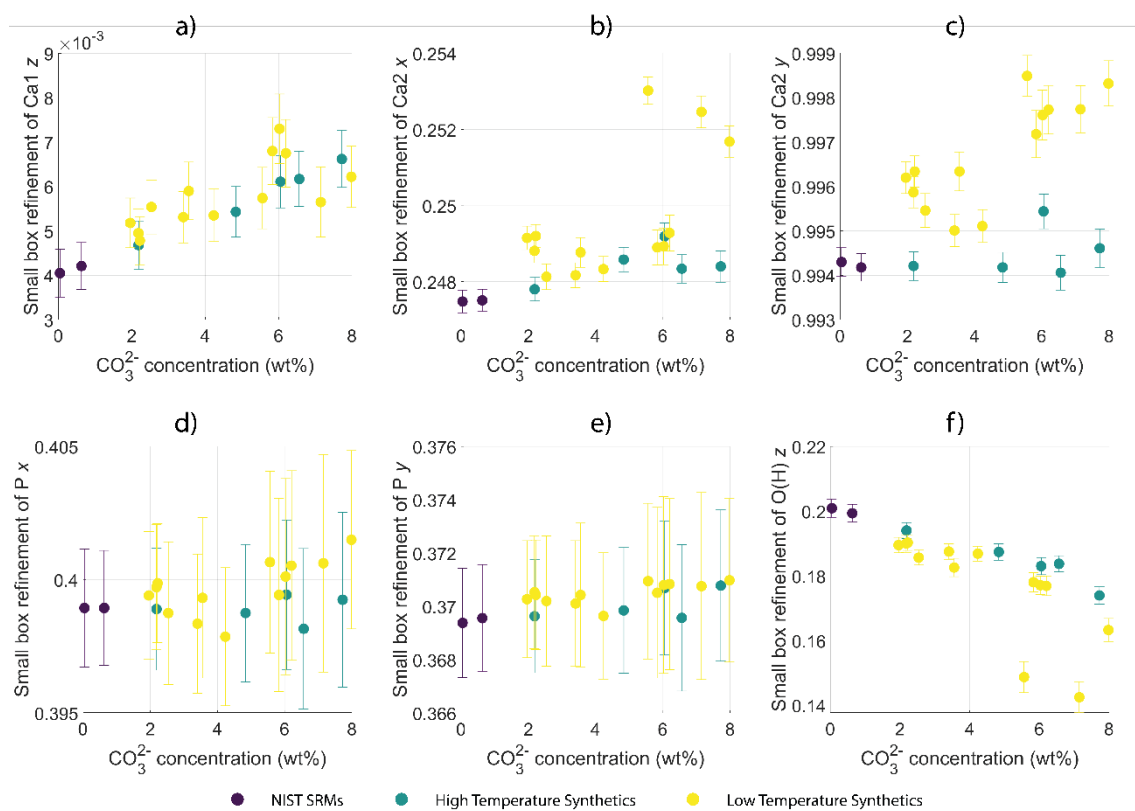


Figure S8 Relationships between atomic fractional coordinates and CO_3^{2-} concentration: *a*) Ca1 z , *b*) Ca2 x , *c*) Ca2 y , *d*) P x , *e*) P y and *f*) O(H) z . Error bars represent fitting errors. Error bars represent estimated standard deviation.

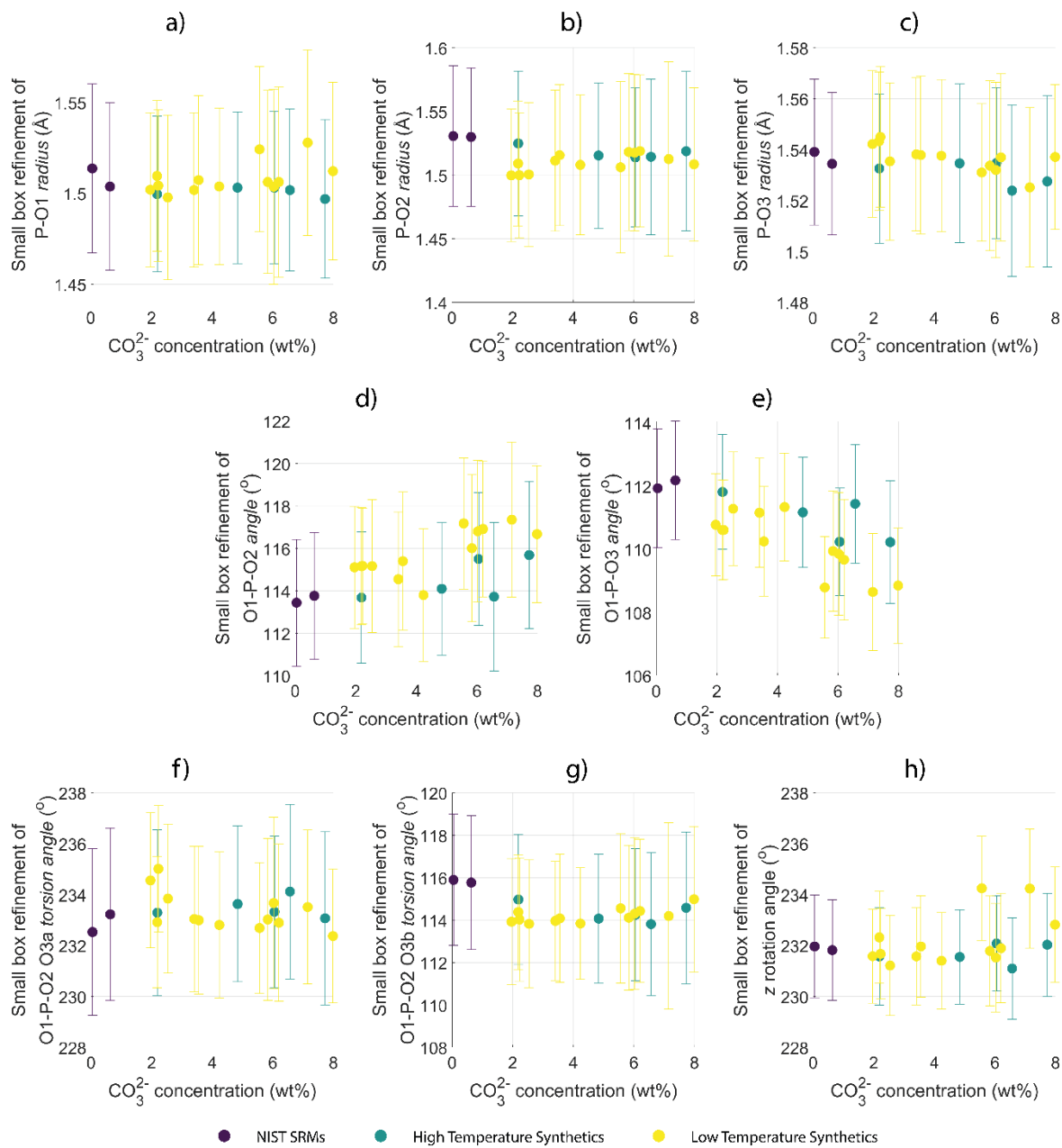


Figure S9 Relationships between rigid body parameters and CO_3^{2-} concentration: *a*) P-O1 bond distance, *b*) P-O2 bond distance, *c*) P-O3 bond distance, *d*) O1-P-O2 angle, *e*) O1-P-O3 angle, *f*) O1-P-O2 O3a torsion angle, *g*) O1-P-O2 O3b torsion angle and *h*) *z* rotation angle. Error bars represent estimated standard deviation.

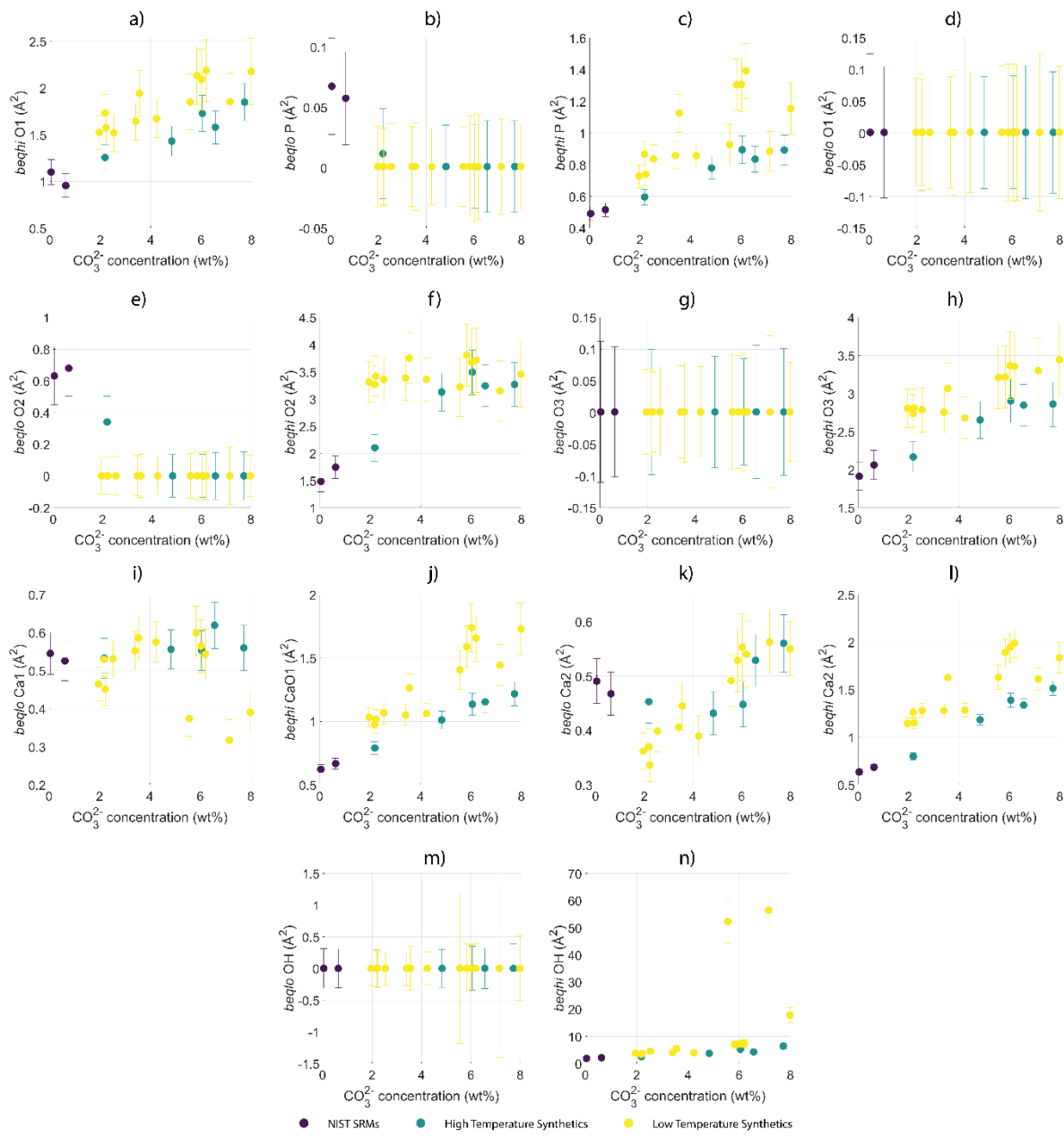


Figure S10 *beq* parameters correlated to total CO_3^{2-} concentration: a) *beqli P*, b) *beqli P*, c) *beqli O1*, d) *beqli O1*, e) *beqli O2*, f) *beqli O2*, g) *beqli O3*, h) *beqli O3*, i) *beqli Ca1*, j) *beqli Ca1*, k) *beqli Ca2*, l) *beqli Ca2*, m) *beqli O(H)* and n) *beqli O(H)*. Error bars represent estimated standard deviation.

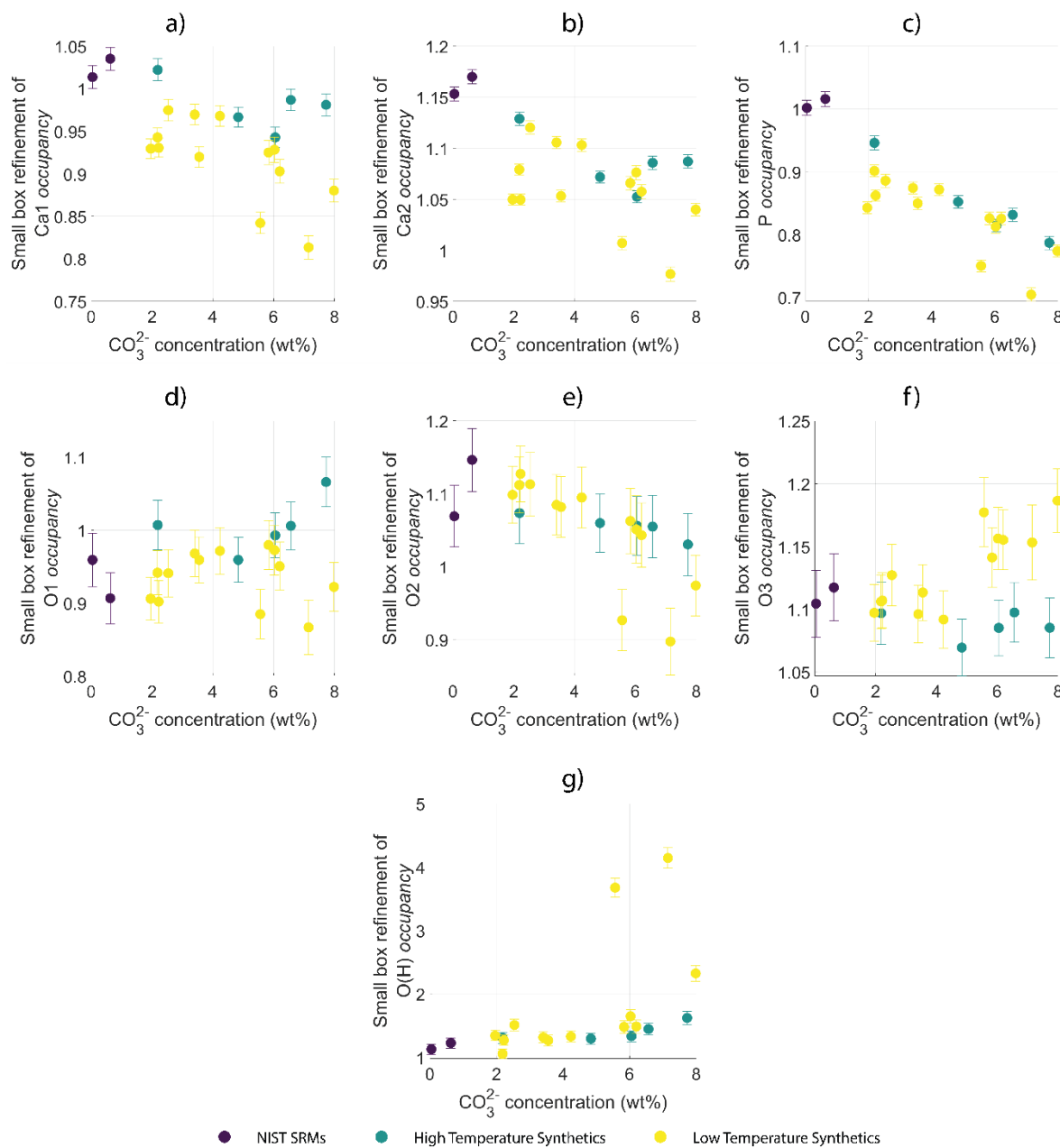


Figure S11 Relationships between occupancy and CO_3^{2-} concentration: *a*) Ca1 occupancy, *b*) Ca2 occupancy, *c*) P occupancy, *d*) O1 occupancy, *e*) O2 occupancy, *f*) O3 occupancy and *g*) O(H) occupancy. Error bars represent estimated standard deviation.